Molecular Neurobiology

ISSN0893-7648/97/15(1): 17–29/$11.25

Acetylcholine and Associative Memory in the Piriform Cortex

Edi Barkai*[*,1] and Michael H. Hasselmo[2]

[1]Department of Physiology, Faculty of Health Sciences and Zlotowski Center for Neuroscience, Ben-Gurion University of the Negev, Beersheva, Israel 84105; and [2]Department of Psychology, Harvard University, Cambridge, MA 02138

Abstract

The significance of cholinergic modulation for associative memory performance in the piriform cortex was examined in a study combining cellular neurophysiology in brain slices with realistic biophysical network simulations. Three different physiological effects of acetylcholine were identified at the single-cell level: suppression of neuronal adaptation, suppression of synaptic transmission in the intrinsic fibers layer, and activity-dependent increase in synaptic strength. Biophysical simulations show how these three effects are joined together to enhance learning and recall performance of the cortical network. Furthermore, our data suggest that activity-dependent synaptic decay during learning is a crucial factor in determining learning capability of the cortical network. Accordingly, it is predicted that acetylcholine should also enhance long-term depression in the piriform cortex.

Index Entries: Piriform cortex; acetylcholine; memory; neuronal adaptation.

Introduction

Rats demonstrate a capacity for memory function in the olfactory modality analogous to memory function for the visual modality in primates (Jenings and Keefer, 1969; Slotnick and Katz; 1974; Staubli et al., 1984, 1986, 1987; Eichenbaum et al., 1986), making it an appropriate model system for studying the neural substrate of memory function. Blockade of muscarinic cholinergic receptors has been shown to impair learning of new information in a wide range of behavioral tasks (Sutherland et al., 1982; Hagan and Morris, 1989; Aigner et al., 1991; Hasselmo, 1994). In particular, antagonists, such as scopolamine, impair the learning of new odors (Hunter and Murray, 1989; Soffie and Lamberty, 1988). However, it is not clear how these behavioral phenomena relate to the physiological effects of acetylcholine (ACh) within cortical structures.

*Author to whom all correspondence and reprint requests should be addressed.

Brain slice preparations provide an ideal substrate for exploring cholinergic-induced changes of the intrinsic properties of neurons, as well as modifications of their synaptic inputs. Piriform cortex slices are of special advantage for investigating synaptic modifications owing to their special anatomical structure, which show clear segregation between cell bodies (layer II), proximal dendrites (layer Ib), which are activated by intrinsic fibers only, and distal dendrites (layer Ia), which contain synaptic terminals of afferent axons only. This anatomical structure allows synaptic activity to be evoked from well-identified pathways.

Realistic computational modeling is a powerful tool that provides the crucial link between cellular events and behavioral phenomena, such as learning. Our work combines electrophysiological recordings from brain slices with single-cell (Fig. 1) and network biophysical modeling to examine how cholinergic effects may be combined to set the proper dynamics for learning in the piriform cortex.

Cellular Effects of ACh on Pyramidal Cells

Suppression of Neuronal Adaptation

Adaptation of firing frequency is commonly found in cortical pyramidal cells (Connors et al., 1982; Madison and Nicoll, 1984; McCormick et al., 1985; Schwindt et al., 1988; Agmon and Connors, 1992). We tested the repetitive firing properties of piriform cortex pyramidal cells using a full range of current injection amplitudes. Although neurons differed markedly in their adaptation rate, certain common characteristics of firing patterns were evident. Injection of current sufficient to depolarize the neuron to threshold potential caused the firing of a single spike. Increasing stimulus intensity resulted in a gradual increase in the number of action potentials evoked. Firing frequency was highest for the first two spikes and decreased gradually as current injection continued. As was previously demonstrated (Madison and Nicoll, 1984; McCormick and Prince, 1986; Tseng and Haberly, 1989), application of the muscarinic agonist carbachol (20 μM) reduced adaptation considerably. Increase in firing frequency was most prominent on the response to the later part of a 1-s injected pulse. Effect on initial firing frequency was notably mild. The adaptation strength of each neuron was examined using a quantitative measure termed S-I value (*see* Barkai and Hasselmo, 1994). This allowed construction of single-cell biophysical models that could imitate "typical" piriform cortex pyramidal neurons in control conditions and when carbachol is applied (Fig. 2).

Suppression of Synaptic Transmission

Carbachol strongly suppresses synaptic transmission in the intrinsic, but not afferent fibers (Hasselmo and Bower, 1992, 1993). This effect is dose-dependent and is probably caused by reducing synaptic release, as indicated by increased paired-pulse facilitation (Hasselmo and Bower, 1992). In the biophysical simulation, reduction of synaptic strength is implemented by reducing the postsynaptic sodium conductance activated by presynaptic activity. Figure 3 shows the effect of carbachol on synaptic transmission in a brain slice and the simulation of its effect in the model. Cholinergic suppression of intrinsic excitatory synaptic transmission has also been demonstrated in somatosensory cortex brain slices (Hasselmo and Cekic, 1996).

Enhancement of Long-Term Potentiation (LTP)

ACh has been demonstrated to enhance the induction of LTP in hippocampal region CA1 (Hirotsu et al., 1989; Tanaka et al., 1989; Blitzer et al., 1990; Huerta and Lisman, 1994) and in the dentate gyrus (Burgard and Sarvey, 1990). This may be related to the cholinergic enhancement of stimulation-initiated protein synthesis via an NMDA-dependent mechanism (Feig

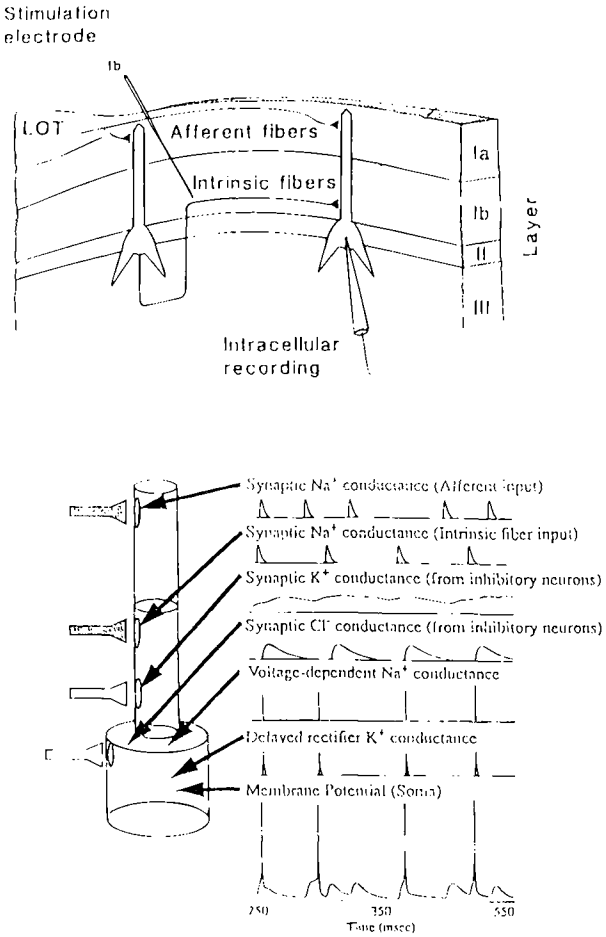

Fig. 1. **(Top)** A schematic representation of the piriform cortex slice preparation. Pyramidal cells receive excitatory afferent input in the distal dendrite from olfactory bulb afferent fibers and excitatory intrinsic input in the proximal dendrite from other cortical pyramidal cells. Stimulating electrodes were placed in layer Ib (intrinsic fiber layer). Extracellular recordings were performed in layer Ib and intracellular recordings from pyramidal cell bodies located in layer II. Experiments were performed on brains removed from etherized female albino Sprague-Dawley rats 4–6 wk of age. Slices of piriform cortex were prepared and maintained following standard procedures (Barkai and Hasselmo 1994). **(Bottom)** Schematic representation of the biophysical simulation of a single piriform cortex pyramidal cell, with two dendritic and one somatic compartment containing a range of synaptic and voltage-dependent conductances. Synaptic conductances shown here include excitatory synaptic sodium conductances in the distal and proximal dendritic compartments,inhibitory potassium conductance in the proximal dendritic compartment, and chloride conductance in the soma. Voltage-dependent conductances include the Hodgkin-Huxley fast sodium and delayed rectifier potassium conductances, which underlie the generation of action potentials in the membrane potential trace. Not shown: Additional calcium and voltage-dependent potassium currents underlying adaptation. (Based on figure in Barkai et al., 1994.)

and Lipton, 1993) and to cholinergic potentiation of NMDA receptor-mediated responses (Markram and Segal, 1990). Stimulating 10 s at 5 Hz does not induce significant LTP of the intrinsic synapse in control conditions, but a substantial increase in synaptic potential is noted if the stimuli are applied in the presence of carbachol (Fig. 4). This LTP cannot be induced when NMDA receptors are blocked (Hasselmo and Barkai, 1995).

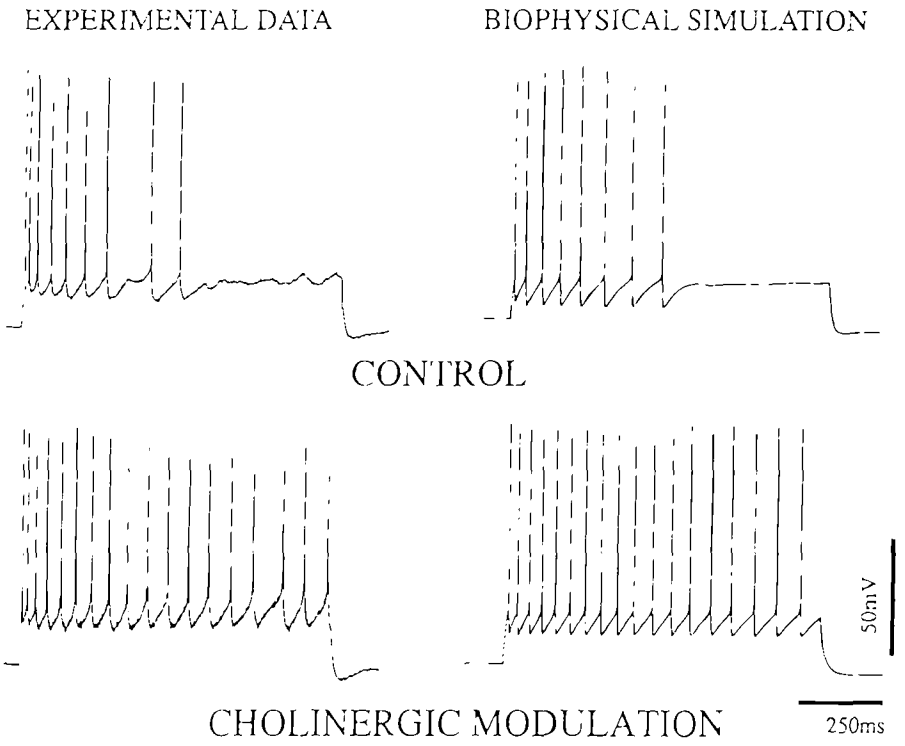

Fig. 2. Intracellular recordings **(left)** and biophysical simulations **(right)** demonstrating suppression of neuronal adaptation induced by carbachol. A 1-s pulse of 0.7 nA was delivered before (upper trace) and during (lower trace) carbachol application. The main effect of the cholinergic agonist is increasing firing rate at the later part of the response. Various levels of adaptation are implemented in the biophysical simulation by calcium-dependent and sodium-dependent conductances. (Taken from Barkai et al., 1994.)

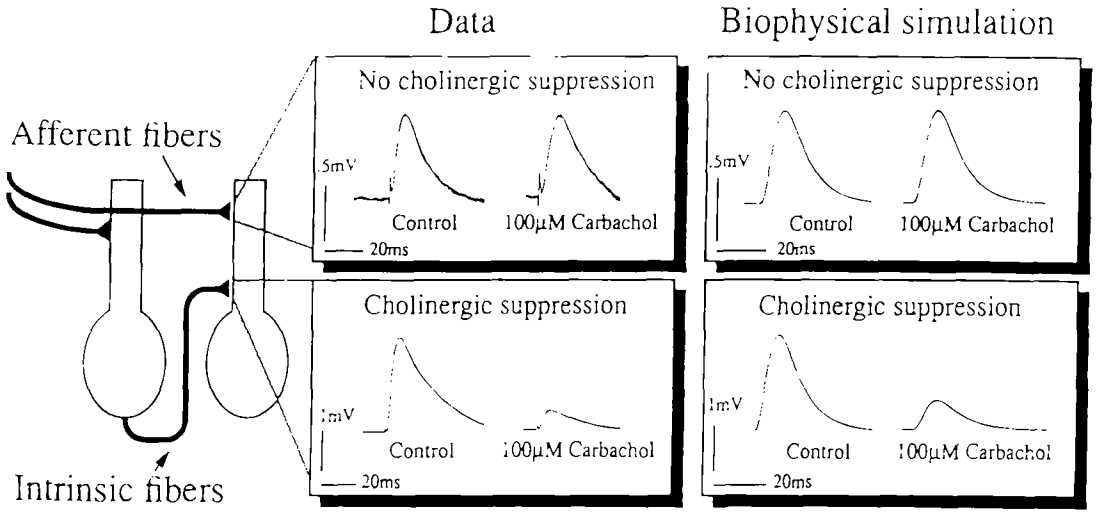

Fig. 3. Selective cholinergic suppression of synaptic transmission is observed in brain slices **(left)** and is implemented in the biophysical model **(right)** by decreasing maximal conductance of synaptically activated sodium channels. (Taken from Barkai et al., 1994.)

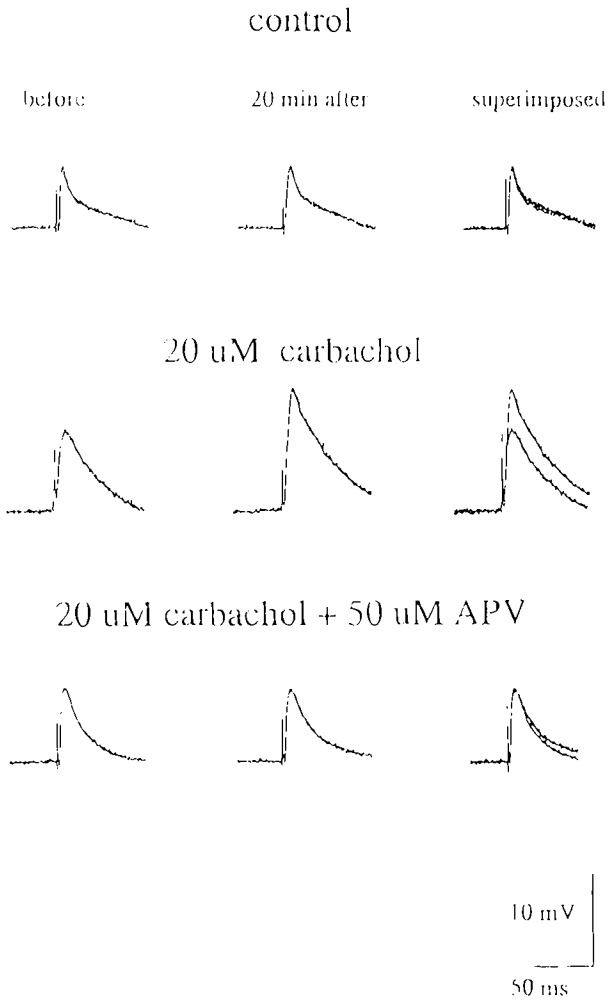

Fig. 4. Activity-dependent synaptic enhancement. **(Top)** Repetitive stimuli applied at 5 Hz for 10 s do not induce LTP under control conditions **(Middle)** Same stimulus paradigm induces LTP in the presence of 20 μ*M* carbachol. **(Bottom)** 50 μ*M* APV prevents LTP induction. Traces are average of 5 EPSPs evoked at 0.1 Hz. Potentials before and 20 min after the 5-Hz stimuli are compared. (*See* Hasselmo and Barkai, 1995.)

Simulating Cholinergic Effects with a Biophysical Network

Computational biophysical simulations of single neurons described above are combined in networks with parameters representing the transmission of action potentials along axons and the conductances mediated by synapses on the dendrites of other neurons. According to piriform cortex anatomy, 240 simulated pyramidal cells receive excitatory afferent input to the distal dendrite and excitatory intrinsic input to the proximal dendrite from intercortical cells (Fig. 5). Each pyramidal cell is connected to 70% of the other pyramidal cells, on average. This unrealistically high percentage is used to compensate for the relatively small size of the network. The model also contains 58 each of inhibitory interneurons mediating feedforward inhibition (receiving excitatory afferent input) and feedback inhibition (receiving excitatory intrinsic input). Both feedforward and feedback inhibition include interneurons activating $GABA_A$ receptors (activating chloride conductance in somatic compartments) and $GABA_B$ receptors (activating potassium conductance in proximal dendritic compartments). Axon transmission delay is calculated based on a computation of the distance between modeled neurons and the experimentally determined transmission delays along those axons. Synaptic currents are represented by shifts in the ionic conductance for Na for excitatory synapses and K or Cl for different inhibitory synapses, with the time-course of synaptic currents following a standard dual exponential time-course with specific time constants dependent on the specific receptor and channel type. Modifications of synaptic strength occur by changing the postsynaptic conductance when the presynaptic cell generates action potentials. Synaptic strength may be enhanced or decreased. Strengthening of synaptic connections occurs when presynaptic activity occurs simultaneously with postsynaptic activity, and synaptic weakening is induced when only the presynaptic cell is activated.

Suppression of Neuronal Adaptation Enhances Learning

Implementing the Hebbian learning rule enables the network to perform associative memory function (Fig. 6). Decreased neuronal adaptation results in increasing the rate of strengthening the excitatory synaptic connection. This effect is a direct result of the increase

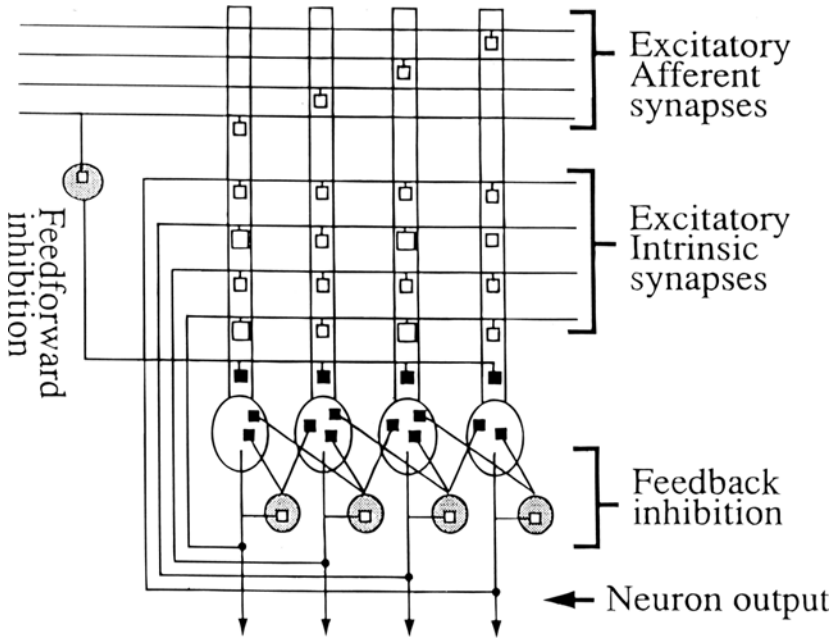

Fig. 5. Network simulation is composed of 240 pyramidal neurons receiving excitatory afferent input on the distal part of their dendrite and excitatory intrinsic input on the proximal portion of the dendrite. Feedforward inhibition (activated by the afferent input) is applied to the distal dendrites and feedback inhibition (activated by the intrinsic synapses) is applied to the cell bodies (*see* Tseng and Haberly, 1988). Fifty-eight inhibitory interneurons from each type are evenly distributed in the network. Synaptic inhibition strength decreases gradually as pyramidal cells are located further from the inhibitory interneurons. (Taken from Barkai et al., 1994.) Excitatory neurons may switch from "strong adapting" mode when control conditions are simulated to "weak adapting" mode when ACh is present. Inhibitory neurons fire at a constant rate without adaptation. Development of single cells and network models is based on previous biophysical simulations, using the GENESIS package (Wilson and Bower 1989, 1992).

in firing rates, especially toward the later part of the training session. Under control conditions, most pyramidal neurons rarely fire action potentials 200 ms after stimulus onset (Barkai and Hasselmo, 1994). Thus, the later part of the 500-ms activation is not efficient for modifying synaptic connections. When ACh is present, the same neurons are capable of generating action potentials throughout the period in which afferent stimulation is present. Consequently, modification of synaptic connections is enhanced. Effect of suppression of neuronal adaptation at a single excitatory synapse is shown in Fig. 7A and on strengthening synaptic connections throughout the network in Fig. 7B.

Suppression of Synaptic Transmission Prevents Runaway Synaptic Modification

Different odorants do not activate orthogonal patterns in the piriform cortex. When presenting a monkey with eight different odors, more then 50% of the neurons in the piriform cortex responded to at least one odor (Tanbe et al., 1975). Efficient learning of overlapping patterns is restricted by the prospects of extending the strength of synaptic connections up to a point at which activity in a subpopulation of neurons that represent a learned pattern will spread into another subpopulation of neurons, which form together a different pattern. This undesired spread of activation, mediated by neurons that

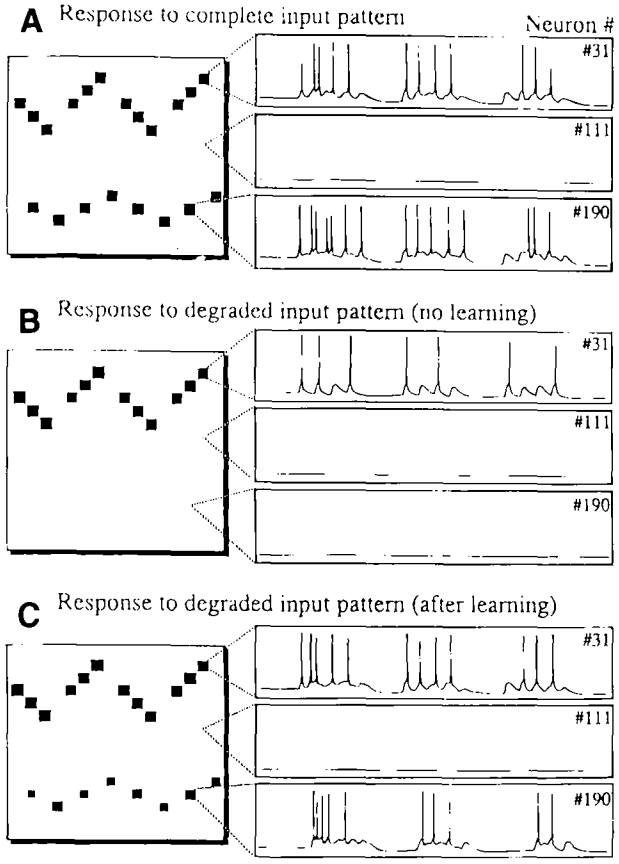

Fig. 6. Neuronal activity during recall. Associative memory function with a single learned pattern in a 240-neuron network biophysical simulation (*see* Barkai et al., 1994). On the left, the size of the black squares represents the number of spikes fired by each of the 240 (in an array of 15 × 16) neurons during recall. On the right, membrane potential traces are shown for three simulated pyramidal cells (numbers 31, 111, and 190) over a period of 600 ms. **(A)** Response of the network to the complete version of the pattern. Twenty neurons show spiking activity owing to activation by the afferent input pattern. On the right, two neurons receiving afferent input generate action potentials, whereas one neuron not receiving input shows only slight inhibitory influences. **(B)** No learning. Response to a degraded version of the pattern when no modification of excitatory intrinsic synapses has occurred. Note that only 12 neurons show spiking activity. Eight neurons are no longer active owing to removal of eight input lines. Because learning has not occurred, these neurons do not receive sufficient excitatory intrinsic input to show completion. On the right, one of the neurons previously receiving afferent input now does not fire. **(C)** Completion after learning. Response to degraded version of the pattern after modification of excitatory intrinsic synapses during learning of the pattern. Note that the eight neurons not receiving the afferent input now fire in response to the spread of activity across strengthened excitatory intrinsic synapses. On the right, the spiking activity of the neuron not receiving afferent input has been restored.

are shared by both patterns, will then advance to other subpopulations, until a large portion of the neurons in the network will fire synchronously. The outcome of such a process is that the network will respond with excessive, broadly distributed activity whenever a learned pattern or a part of it is presented. The hyperexcitable response does not discriminate between different input lines and is very different from all the learned patterns (Fig. 8). Thus, the seemingly paradoxical suppression of excitatory transmission by ACh is essential to prevent a

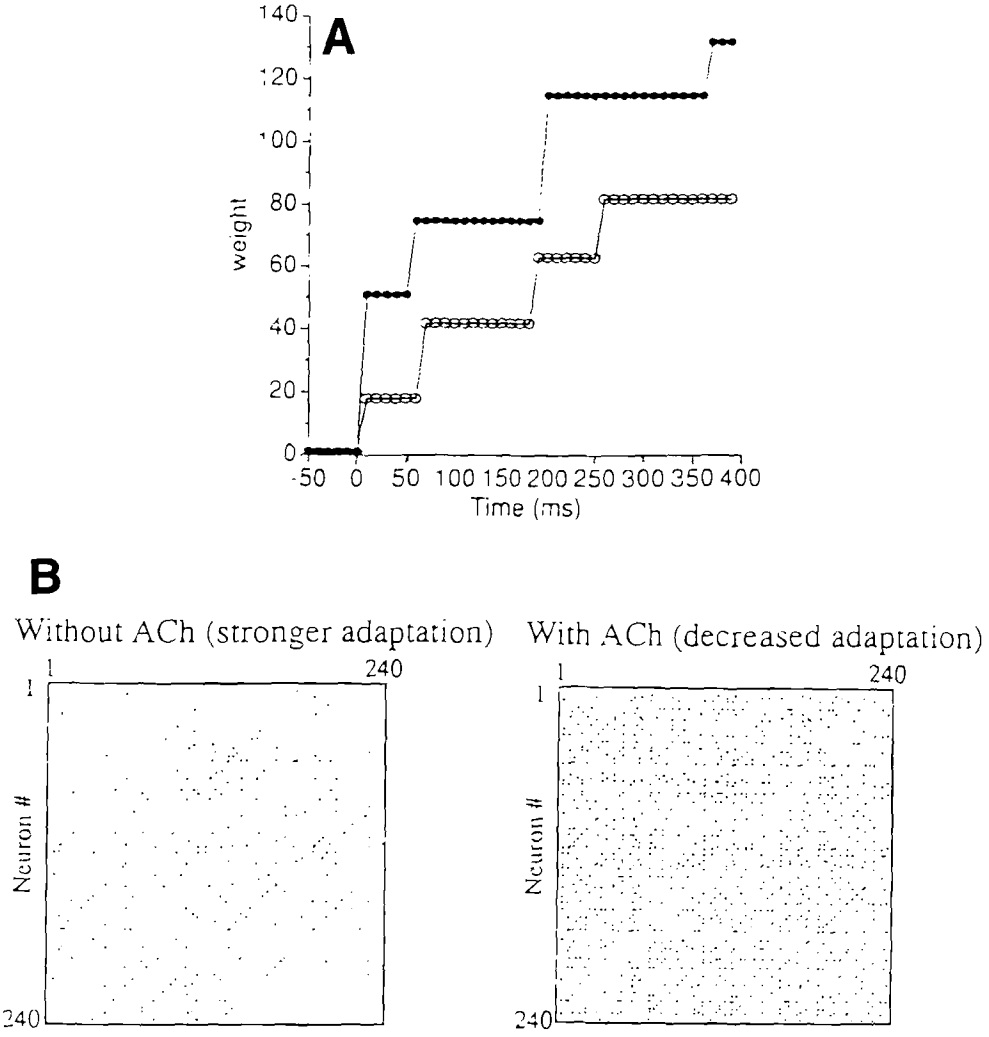

Fig. 7. Suppression of neuronal adaptation enhances learning in the biophysical network simulation. **(A)** Rate of learning in a single excitatory synapse is higher when the network is composed from neurons with weaker adaptation (closed circles) than in a network that contains neurons that adapt strongly (open circles). **(B)** Synaptic connectivity matrixes, showing strength of connectivity among all pyramidal cells in the network. Training the network when neurons have weaker adaptation allows many connections to be enhanced to their maximal possible value.

nonspecific excitation that causes runaway synaptic modification, which prevents the network from performing associative memory.

Activity-Dependent Synaptic Enhancement Alone Is Not Efficient

Activity-dependent enhancement of synaptic connections can provide good recall of the stored pattern, but excessive strengthening of intrinsic synapses can lead to simultaneous recall of all stored patterns, resulting in a loss of discrimination between patterns. As shown in Fig. 9, different learning rates result in different performances of the associative memory function. When a low rate was used, the network was unable to perform associative memory function, since connections between pyramidal cells were not sufficiently strengthened during the learning mode to allow a spread of activity

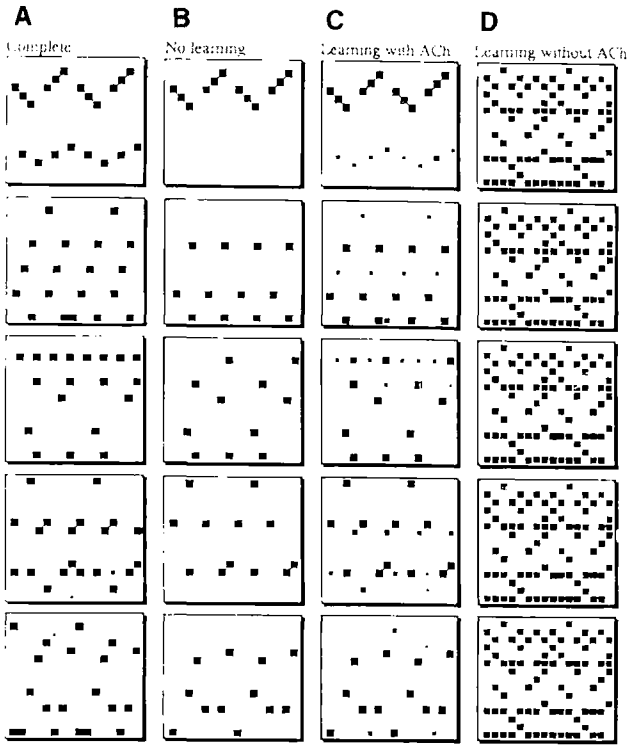

Fig. 8. Suppression of synaptic transmission enables storage of overlapping patterns. The spiking activity of each of the 240 pyramidal cells is shown in different conditions, with the size of the black squares representing the number of action potentials fired during a 500-ms period. **(A)** Response to the complete versions of five different patterns. Each pattern activated 20 pyramidal cells. Each two patterns overlapped by 10%, and the total overlap between all was 50%. **(B)** Response to a degraded versions of the input pattern (missing eight input lines each) before any learning has occurred. **(C)** Response to degraded versions of the input pattern after learning in the presence of cholinergic effects. Note that the spread of activity across previously modified intrinsic synapses causes spiking activity in neurons, which were elements of the complete learned pattern. **(D)** Response to the degraded versions of the input pattern after learning without cholinergic suppression of synaptic transmission. Excessive strengthening of intrinsic synapses results in recall of elements of all the patterns stored in the network, preventing discrimination among different patterns. (Taken from Barkai et al., 1994.)

in the network during the recall mode. Therefore, when the partial patterns were presented during recall, the spiking response of the network was incomplete in comparison to the response to the full pattern. When the learning rate was increased to an ideal value, the network was capable of completing some of the missing inputs. When the learning rate was further increased, the network entered an hyperexcitable state, in which it ceased to discriminate between different patterns. Figure 9 also describes quantitatively the relationship between learning rate and the performance of the network. It is evident that for the period of learning utilized in these simulations only, a narrow range of learning rates was suitable for allowing completion specific to individual patterns.

Activity-Dependent Long-Term Synaptic Depression During Learning Increases the Network's Stability

The narrow range of learning rates that result in good recall introduces an interesting question: How can the proper rate of synaptic modification be obtained within the actual

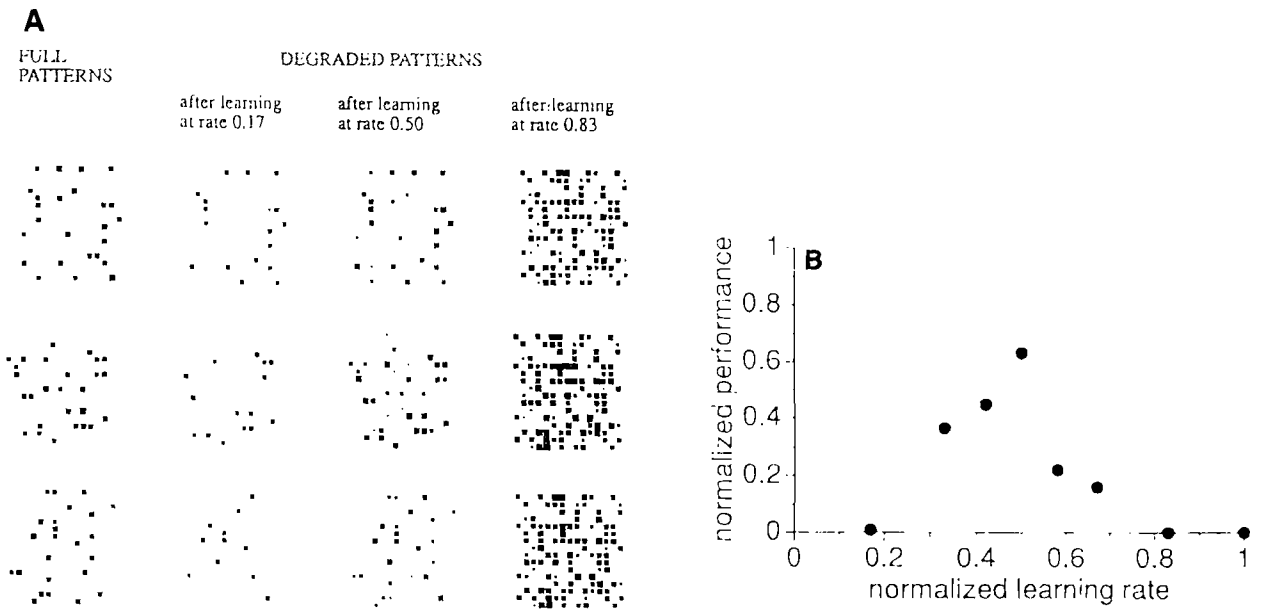

Fig. 9. Effects of different learning rates on performance of associative memory function. **(A)** Learning rates were normalized to the rate needed to bring a synapse to its possible maximum strength when pre- and postsynaptic neurons are activated synchronously for 600 ms. The first column illustrates three of the five patterns of activity that were learned by the network. The size of the black squares represents the number of spikes fired by each of the 240 simulated piriform cortex pyramidal cells. Each pattern was generated by activating two afferent input fibers, which causes broadly distributed activity in the pyramidal cells. The average percentage of connections between the afferent fibers and the pyramidal cells was 5%. Columns 2–4 represent the activity generated by the network in response to activating only one of the afferent fibers of each pattern. In the second column, responses are shown after learning at a rate that was 17% (0.17) of the rate that would drive all active connections to their maximal possible weight. After learning at this rate, the network was not capable of performing completion of degraded patterns. In the third column, responses to degraded patterns after learning at a rate that was 50% (0.5) of the maximal rate are shown. Here, strengthening of intrinsic connections allows completion of missing elements of the degraded pattern (compare with column 1). In the fourth column, responses for degraded patterns after learning at a rate that was 83% (0.83) of the maximal rate show spread of activity to a large portion of the network. Responses are very different from the original patterns and are similar to each other, reflecting the loss of discrimination between patterns. **(B)** Graph showing the normalized performance measure as a function of the normalized learning rate (*see* Barkai et al., 1994 for normalized performance measurements). Effective recall may be obtained only when applying learning rates in the lower range. (Modified from Hasselmo and Barkai, 1995.)

neural ensemble? This suggests that even if the correct learning rate is applied when an individual memory is stored, these synaptic connections might still be excessively strengthened when additional patterns are presented. A common response to this difficulty in more abstract models of cortical function has been to incorporate normalization of synaptic strength or activity-dependent depression of synaptic strength (Grossberg, 1972; Levy et al., 1990). We examined the possibility that activity-dependent depression in the strength of synaptic connectivity may offer a solution to this problem in the network biophysical simulation.

The effect of introducing a depression rate into the system on the synaptic connectivity matrix is shown in Fig. 10. Note the difference in efficacy of applying depression during learning and during recall. Although introducing depression during recall does not significantly improve associative memory performance, applying the depression rule during learning re-

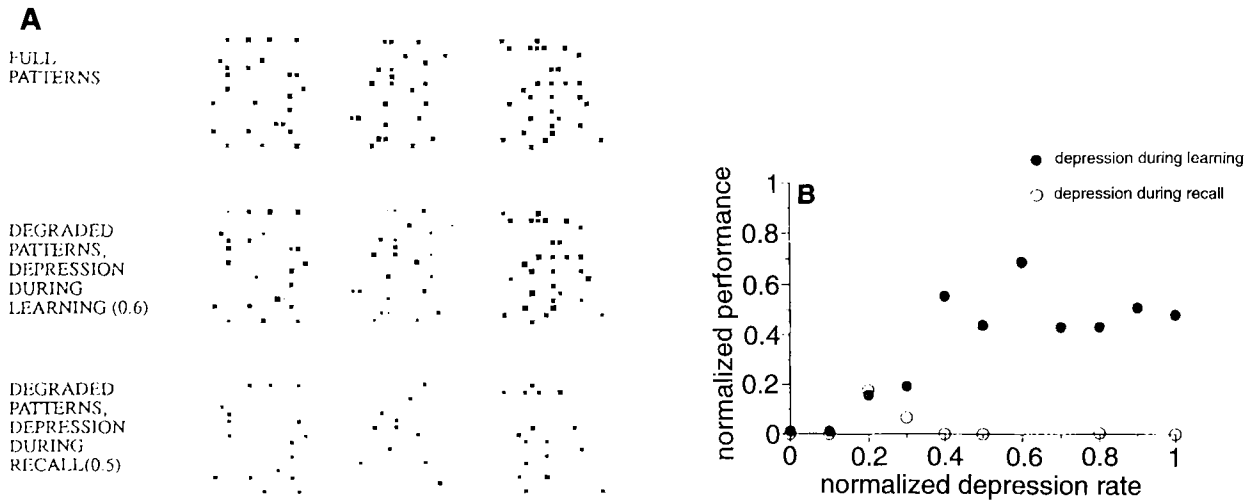

Fig. 10. Recall performance in the model after applying depression during learning and during recall. **(A)** In the first row, three out of five full patterns are represented (same patterns as in Fig. 9). The second row illustrates the completion ability of a network in which a learning rate of 1.0 was combined with a depression rate of 0.6 during learning (for determination of depression rate, *see* Hasselmo and Barkai, 1995). The responses to three degraded patterns are shown (degraded patterns are the same as in Fig. 9, column 2). The third row shows that applying a depression rate of 0.5 during recall after training with a learning rate of 1.0 does not allow completion of the patterns. **(B)** Graph showing the normalized performance measure during recall as a function of the depression rate during learning (full circles) and during recall (empty circles). A learning rate of 1.0 was applied. No depression rate is efficient when applied after learning. In contrast, when depression is applied during learning, all depression rates with values of 0.4 or more are efficient in improving recall performance considerably. These results suggest that synaptic depression should be enhanced at the same time as synaptic strengthening.

sulted in a steady improvement of memory, with a similar level of improvement across a range of depression values from 0.4 to 1.0.

Simulations with the biophysical network suggest that the depression process should take place during learning rather than during recall in order to be effective. In other words, the network simulation indicates that a "forgetting" process should occur simultaneously with the learning process, rather than afterward. This leads to the prediction that the depression of synaptic strength should be stronger when cholinergic modulation is present compared with control conditions. Whether this prediction is valid is yet to be explored.

References

Agmon A. and Connors B. W. (1992) Correlation between intrinsic firing patterns and thalamocortical synaptic responses of neurons in mouse barrel cortex. *J. Neurosci.* **12**, 319–329.

Aigner T. G., Walker D. L., and Mishkin M. (1991) Comparison of the effects of scopolamine administrated before and after acquisition in a test of visual recognition memory in monkeys. *Behav. Neural Biol.* **55**, 61–67.

Barkai E. and Hasselmo M. E. (1994) Modulation of the input/output function of rat piriform cortex pyramidal cells. *J. Neurophysiol.* **72**, 644–658.

Barkai E., Bergman R., Horwitz G., and Hasselmo M. E. (1994) Modulation of associative memory function in a biophysical simulation of rat piriform cortex. *J. Neurophysiol.* **72**, 659–677.

Blitzer R. D., Gil O., and Landau E. M. (1990) Cholinergic stimulation enhances long-term potentiation in the CA1 region of rat hippocampus. *Neurosci. Lett.* **119**, 207–210.

Burgard E. C. and Sarvey J. M. (1990) Muscarinic receptor activation facilitates the induction of long-term potentiation (LTP) in the rat dentate gyrus. *Neurosci. Lett.* **116**, 34–39.

Connors, B. W., Gutnick, M. J., and Prince D. A. (1982) Electrophysiological properties of neocortical neurons in vitro. *J. Neurophysiol.* **48**, 1302–1320.

Eichenbaum H., Fagan A., and Cohen N. J. (1986) Normal olfactory discrimination learning set and facilitation of reversal learning after medial-temporal damage in rats: implications for an account of preserved learning abilities in amnesia. *J. Neurosci.* **6(7)**, 1876–1884.

Feig S. and Lipton P. (1993) Pairing the cholinergic agonist carbachol with patterned schaffer collateral stimulation initiates protein synthesis in hippocampal CA1 pyramidal cell dendrites via a muscarinic, NMDA-dependent mechanism *J. Neurosci.* **13(3)**, 1010–1021.

Grossberg S. (1972) Some networks that can learn, remember and reproduce any number of complicated space-time patterns. II. *Stud. Appl. Math.* **49**, 135–166.

Hagan J. J. and Morris R. G. M. (1989) The cholinergic hypothesis of memory: a review of animal experiments, in *Psychopharmacology of the Aging Nervous System* (L. L. Iversen and S. H. Snyder, eds.) Plenum, New York pp. 237–324.

Hasselmo M. E. (1994) Neuromodulation and cortical function: modeling the physiological basis of behavior. *Behav. Brain Res.*, in press.

Hasselmo M. E. and Barkai E. (1995) Cholinergic modulation of activity-dependent synaptic plasticity in the piriform cortex. *J. Neurosci.* **15(10)**, 6592–6604.

Hasselmo M. E. and Bower J. M. (1992) Cholinergic suppression of specific to intrinsic not afferent fibers in rat piriform (olfactory) cortex. *J. Neurophysiol.* **67(5)**, 1222–1229.

Hasselmo M. E. and Bower J. M. (1993) Acetylcholine and memory. *Trends Neurosci.* **16**, 218–222.

Hasselmo M. E. and Cekic M. (1996) Suppression of synpatic transmission may allow the combination of associative feedback and self-organized feed forward connections in the neocortex. *Behv. Brain. Res.* **79**, 153–161.

Hirotsu I., Hori N., Katsuda N., and Ishihara T. (1989) Effect of an anticholinergic drug on longterm potentiation in rat hippocampal slices. *Brain Res.* **482**, 194–197.

Huerta P. T. and Lisman J. E. (1994) Heightened synaptic plasticity of hippocampal CA1 neurons during a cholinergically induced rhythmic state. *Nature* **364**, 723–725.

Hunter A. J. and Murray T. K. (1989) Cholinergic mechanisms in a simple test of olfactory learning in the rat. *Psychopharmacology* **99**, 270–275.

Jenings J. W. and Keefer L. H. (1969) Olfactory learning set in two varieties of domestic rat. *Psychology Rep.* **24**, 3–15.

Levy W. B., Colbert C. M., and Desmond N. L. (1990) Elemental adaptive processes of neurons and synapses: a statistical/computational perspective, in *Neuroscience and Connectionist Theory* (Gluck M. A. and Rumelhart D. E., eds.) Erlbaum, Hillsdale, NJ, pp. 187–236.

Madison D. V. and Nicoll R. A. (1984) Voltage clamp analysis of cholinergic action in the hippocampus. *J. Physiol.* **354**, 319–331.

Markram H. and Segal M. (1990) Long-lasting facilitation of excitatory postsynaptic potentials in rat hippocampus by acetylcholine. *J. Physiol.* **427**, 381–393.

McCormick D. A. and Prince D. A. (1986) Mechanisms of action of acetylcholine in the guineapig cerebral cortex in vitro. *J. Physiol.* **375**, 169–194.

McCormick D. A., Connors B. W., Lighthall J. W., and Prince D. A. (1985) Comparative electrophysiology of pyramidal and sparsely spiny stelate neurons of the neocortex. *J. Neurophysiol.* **54**, 782–806.

Schwindt P. C., Spain W. J., Foehring R. C., Stafstorm C. E., Chubb M. C., and Crill W. E. (1988) Slow conductances in neurons from cat sensorimotor cortex and their role in slow excitability changes. *J. Neurophysiol.* **59**, 450–467.

Slotnik B. M. and Katz H. M. (1974) Olfactory learning-set formation in rats. *Science*, **185**, 796–798.

Soffie M. and Lamberty Y. (1988) Scopolamine effects on juvenile on specific recognition in rats: possible interaction with olfactory sensitivity. *Behav. Processes* **17**, 181–190.

Staubli U., Ivy G., and Lynch G. (1984) Hippocampal denervation causes rapid forgetting of olfactory information in rats. *Proc. Natl. Acad. Sci. USA* **81**, 5885–5887.

Staubli U., Fraser D., Kessler M., and Lynch G. (1986) Studies on retrograde and anterograde amnesia of olfactory memory after denervation of the hippocampus by entorhinal cortex lesions. *Behav. Neural Biol.* **46**, 432–444.

Staubli U., Fraser D., Farady R., and Lynch G. (1987) Olfaction and the "data" memory system in rats. *Behav. Neurosci.* **101(6)**, 757–765.

Sutherland R. J., Wishaw I. Q., and Regehr J. C. (1982) Cholinergic receptor blockade impairs spatial localization by use of distal cues in the rat. *J. Comp. Physiol. Psychol.* **96**, 563–573.

Tanabe, Y., Iino, M. and Takagi, S. F. (1975) Discrimination of odors on olfactory bulb pyriform-amygdaloid areas and orbitofrontal cortex of the monkey. *J. Neurophysiol.* **38**, 1284–1296.

Tanaka Y., Sakurai M., and Hayashi S. (1989) Effect of scopolamine and HP 029, a cholinergic inhibitor, on long-term potentiation in hippocampal slices of the guinea pig. *Neurosci. Lett.* **98**, 179–183.

Tseng G. F. and Haberly L. B. (1988) Characterization of synaptically mediated fast and slow inhibitory processes in the piriform cortex in an in vitro slice preparation, *J. Neurophysiol.* **59**, 1352–1376.

Tseng G. F. and Haberly L. B. (1989) Deep neurons in piriform cortex. II. Membrane properties that underlie unusual synaptic responses. *J. Neurophysiol.* **62**, 386–400.

Wilson M. A. and Bower J. M. (1989) The simulation of large-scale neuronal networks, in *Methods in Neuronal Modeling: From Synapses to Networks* edited by Koch C. and Segev I. MIT, Cambridge, MA, pp. 291–334.

Wilson M. A. and Bower, J. M. (1992) Cortical oscillations and temporal interactions in a computer simulation of piriform cortex. *J. Neurophysiol.* **67**, 981–995.